Examination of phase retrieval algorithms for patterned EUV mask metrology

Rene A. Claus[a], Yow-Gwo Wang[b], Antoine Wojdyla[c], Markus P. Benk[c], Kenneth A. Goldberg[c], Andrew R. Neureuther[b], Patrick P. Naulleau[c]

[a]Applied Science and Technology, University of California, Berkeley;
[b]Electrical Engineering and Computer Sciences, University of California, Berkeley;
[c]Center for X-ray Optics, Lawrence Berkeley National Laboratory

ABSTRACT

We evaluate the performance of several phase retrieval algorithms using through-focus aerial image measurements of patterned EUV photomasks. Patterns present a challenge for phase retrieval algorithms due to the high-contrast and strong diffraction they produce. For this study, we look at the ability to correctly recover phase for line-space patterns on an EUV mask with a TaN absorber and for an etched EUV multilayer phase shift mask. The recovered phase and amplitude extracted from measurements taken using the SHARP EUV microscope at Lawrence Berkeley National Laboratory is compared to rigorous, 3D electromagnetic simulations. The impact of uncertainty in background intensity, coherence, and focus on the recovered field is evaluated to see if the algorithms respond differently.

Keywords: Extreme Ultraviolet Lithography, Phase Retrieval, Phase Shift Mask, Photomasks

1. INTRODUCTION

Phase retrieval algorithms use aerial image measurements to calculate a scalar electric field representation of the object. This field can then be used to simulate aerial images under various imaging conditions including aberrations and different illumination conditions. In photomask inspection, this can be useful when evaluating the printability of defects and planning repairs. Since simulations using the recovered electric field can emulate the optics of the lithography system, phase retrieval may help to provide a more accurate estimate of printability. Alternatively, the process window impact of a defect can be computed by simulation instead of by imaging the defect through the entire process window, potentially saving time.

An important challenge to the use of phase retrieval in photomask inspection is that some algorithms perform poorly on the high contrast, strongly diffracting patterns found on photomasks.[1] Low contrast patterns such as Extreme Ultraviolet (EUV) multilayer defects have already been successfully imaged.[2] There are many available methods for phase retrieval from defocused images; however, the phase retrieval problem is nonlinear, so the performance of a given algorithm generally depends on the object.

To examine the performance on patterned masks, we examine three phase retrieval algorithms using different approaches. The Gerchberg-Saxton[3] (GS), Transport of Intensity[4] (TIE), and Weak Object Transfer Function[5] (WOTF) are applied to aerial image measurements of two different EUV photomasks. One mask uses a standard TaN absorber and the other is an etched multilayer mask. The measurements were performed on the actinic zoneplate microscope, SHARP, at Lawrence Berkeley National Laboratory.[6] Since the measurements are not perfect, we examine what impact three common measurement errors would have on the recovered field. We look at the impact of background intensity, coherence, and a focus offset.

Further author information: (Send correspondence to Rene A. Claus)
Rene A. Claus: E-mail: reneclaus@gmail.com, Telephone: 1 949 334 7363

Photomask Technology 2015, edited by Naoya Hayashi, Bryan S. Kasprowicz, Proc. of SPIE
Vol. 9635, 96350F · © 2015 SPIE · CCC code: 0277-786X/15/$18 · doi: 10.1117/12.2197868

2. EVALUATED ALGORITHMS

We evaluate three algorithms that rely on different approaches and approximations. The Gerchberg-Saxton (GS) algorithm was selected as an example of algorithms that use optimization to find the electric field that best describes the measurements. They use the full, non-linear model. A linearized algorithm based on the Weak Object Transfer Function was tested because it could allow the use of complex illuminations and incorporate aberration models, making it useful for pattern mask measurements. The third algorithm uses the Transport of Intensity Equation (TIE), which uses an approximation of a small defocus distance.

2.1 Gerchberg-Saxton

The GS algorithm,[3] like other optimization-type algorithms uses a current estimate of the electric field and then attempts to improve that estimate to better match the measurements. Several algorithms use different optimization methods but also rely on improving an initial electric field estimate.[7,8] In GS, the current estimate of the electric field is propagated to the image plane corresponding to one of the measurements. The amplitude at that plane is then replaced with the square root of the intensity. The field is then propagated to the next image and forced to match that intensity. In this way the algorithm iteratively forces the field to produce the correct intensity at each measurement. We initialize the electric field using the square root of the intensity at focus and use a constant phase. The advantages of this algorithm are that it is simple, fast, and is guaranteed to converge (though it may only find a local minimum instead of the global minimum). The key characteristic of GS compared to the other algorithms we consider is that it doesn't use any approximations to the imaging equations and that it optimizes an initial estimate to minimize the residual error.

2.2 Weak Object Transfer Function

The WOTF can be used to calculate the electric field from a collection of aerial images when the 0^{th} diffracted order contains most of the energy.[5] If the other diffracted orders are relatively weak, the aerial image can be well described by Eq. 1,

$$I = 1 + E_{re} * K_{re} + E_{im} * K_{im} + I_e \tag{1}$$

$$\widetilde{K_{re}} = \left(\widetilde{P}\cdot\widetilde{J}\right)\star\widetilde{P} + \widetilde{P}\star\left(\widetilde{P}\cdot\widetilde{J}\right) \tag{2}$$

$$\widetilde{K_{im}} = \left(\widetilde{P}\cdot\widetilde{J}\right)\star\widetilde{P} - \widetilde{P}\star\left(\widetilde{P}\cdot\widetilde{J}\right). \tag{3}$$

In this equation, the electric field is assumed to be normalized so that it can be expressed as $E = 1+E_{re}+iE_{im}$. $\widetilde{P}$ is the pupil function, $\widetilde{J}$ is the illumination source shape and I_e is the intensity term corresponding to $|E_{re}+iE_{im}|^2$. If the 0^{th} order is strong enough, this term can be neglected and the equation becomes linear. In situations where the approximation is not sufficiently accurate, the algorithm can be improved by iteratively subtracting an estimate of I_e and recalculating E. Since the algorithm relies on having a dominant 0^{th} order, it is less reliable for patterned masks that have strong diffracted orders. It has the advantage, however, of being able to handle arbitrary source shapes and aberrations.

2.3 Transport of Intensity Equation (TIE)

When the defocus distances between two images is small, the imaging equations can be approximated by the Transport of Intensity Equation,[4,9]

$$\frac{dI}{dx} = -\frac{1}{k}\nabla\cdot(I(z=0)\nabla\varphi). \tag{4}$$

This equation describes how images propagate over small distances. The derivative of intensity over z (focus) can be approximated by a finite difference of two images near focus, allowing the equation to be inverted using two or three images. Typically three images are used where one in-focus image is used as $I(z=0)$ and the two closest images are used to compute $dI/dz \approx \Delta I/\Delta z$. The equation can then be solved for the phase.

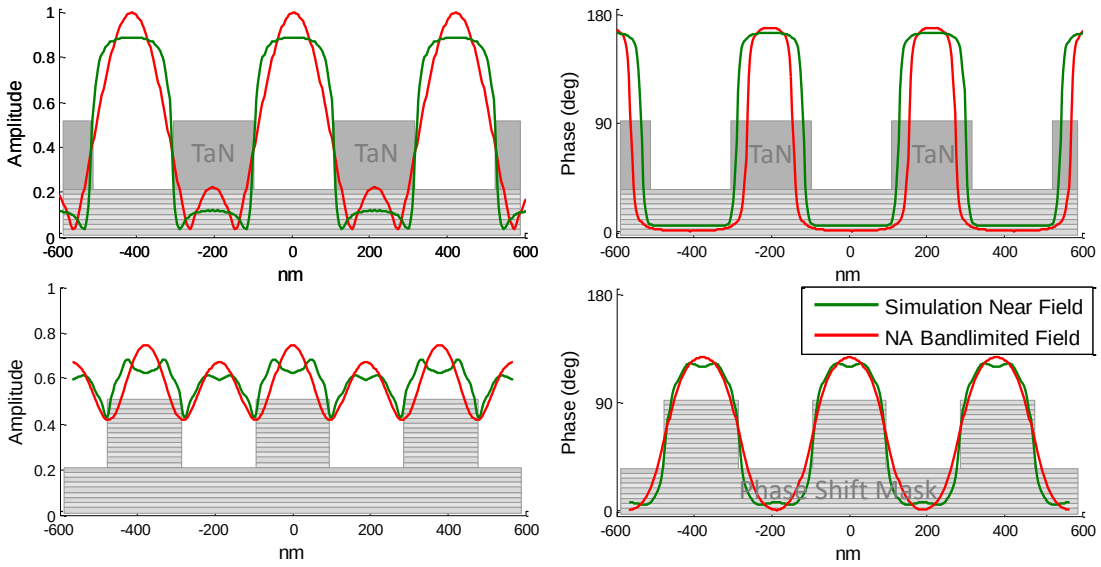

Figure 1: The amplitude and phase of the near field are shown for both the TaN and the phase shift mask. The measurable field is limited by the NA of the system. This low-pass filtered field (NA Bandlimited Field) is what should be recovered from the measurements.

3. TEST OBJECTS

To evaluate how the phase retrieval algorithms perform, two types of masks are considered. Both are EUV masks with a standard multilayer stack of 40 Mo/Si bilayers. The first has a patterned TaN absorber (height = 60 nm) while the second is a phase shift mask. The phase shift mask consists of 12 Mo/Si bilayers that have been etched to create the pattern. For the TaN absorber the pattern examined is a 1:1 line-space pattern with a 200 nm mask-side half pitch (50 nm at the wafer). The pattern is oriented vertically so that the incident beam at 6° will not cause shadowing. The illumination is coherent. Using available data, the phase shift mask had a checkerboard pattern of the same pitch. The patterns on both masks have a large phase shift close to 180°, but the TaN absorber has strong absorption and is used to test the effect of high contrast. The phase shift mask has low absorption which tests the effect of a suppressed 0^{th} order. The phase shift mask is expected to be the most challenging for the phase retrieval algorithms because it has complicated through-focus behavior. The WOTF is expected to struggle because the 0^{th} order is suppressed. GS may perform worse because the initial estimate is further from the correct answer. TIE may struggle with the sharper zeros between phase regions.

To evaluate the performance of the algorithms, a reference to compare to is needed. The phase retrieval results can then be compared to the reference to determine whether the recovered field is accurate. This reference is calculated using rigorous 3D simulations in Hyperlith (using RCWA and 1D features).[10] Figure 1 shows the phase and amplitude of the near field calculated by the simulation. Due to memory limitations, 2D simulations of the checkerboard pattern used for the phase shift mask are unreliable, so as an approximation a 1D simulation is used instead. This will contribute an error to the comparison of the simulation to experimental measurements. The images used for phase retrieval are limited by the numerical aperture (NA) of the microscope, however. This means that the complete near field is not measured and cannot be recovered completely. Instead, a bandlimited version of the near field is a more accurate reference to compare with the phase retrieval result. This bandlimited field is what should match the recovered field if the phase retrieval is successful and the simulation is accurate.

3.1 Experimental Measurements

To evaluate the algorithms, through-focus measurements of a TaN absorber mask and an EUV phase shift mask were performed. A subset of these measurements are shown in Figure 2. The images were captured with an NA = 0.33/4 and coherent illumination. Fifteen images were captured with a focus spacing of 500 nm giving a focus range of ±3.5 µm. This spacing was determined by the stage precision of the tool. For the TIE only

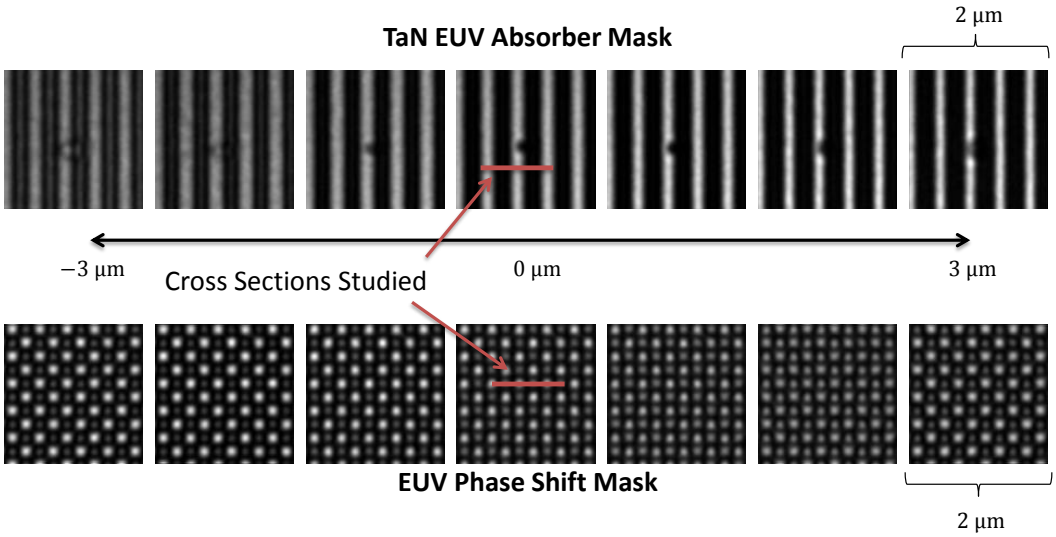

Figure 2: The measurements taken on SHARP are shown. For the TaN absorber the pattern is vertical line space patterns, oriented so that there is no shadowing. The phase shift mask consists of a checkerboard pattern. The cross-section examined is also in the no shadowing direction. The complete data set had 15 images in the range ±3 µm. The images have a width of 2 µm (mask scale).

the central three images were used giving a range of ±500 nm. The TaN absorber mask contained programmed defects, but the region we examined was away from the defect, making it the same as the simulated 1D pattern. For the phase shift mask a horizontal cross section was examined to approximately match the line-space pattern examined for the TaN absorber.

Figure 3 shows the recovered field along the cross-section marked in Figure 2 as calculated by the three algorithms. For the TaN absorber, GS and the WOTF produced very similar fields. This suggests that the answer describes the measurements and is probably not dominated by artifacts due to the recovery. The Transport of Intensity Equation, however, produced a considerably different phase. This could be because TIE only uses 3 images instead of the full 15 images used by the other algorithms, making it more sensitive to noise. The low intensity in the images can also cause the TIE solver to struggle due to the $I(z = 0)$ term in Eq. 4.

For the phase shift mask, the WOTF, in addition to TIE, failed to produce a reasonable result. Unlike for the TaN absorber, it is not possible to say that one recovered field is more accurate due to a match between two algorithms. Instead, using the residual error to compare the WOTF result and the GS result, it is more likely that the GS result is more accurate. The worse performance of the WOA on the phase shift mask is expected since the phase shift mask has a suppressed 0^{th} order and the WOA relies on the 0^{th} order to work.

Instead of using the residual error or a comparison of the different results to evaluate how accurate the recovery is, the result can be compared to the bandlimited near field calculated by simulation. A comparison of the GS result and the simulation is shown in Figure 4. The recovered field and simulation for the TaN absorber match well. The corners of the phase are less square in the recovered phase than expected, but this could be due to a mismatch between the simulation and the physical mask. For example, the simulation assumed perfectly vertical sidewalls, which may not be true. The amplitude minima also do not match up. This could be due to a difference in pixel size in the simulation compared to the experimental results. The simulation pixels are 3.36 nm while the measurements have 15 nm pixels. This is expected to perform a slight low-pass filtering that might explain those minima.

The results for the phase shift mask, on the other hand, are not as good a match. This is likely a combination of the simulation not matching the physical mask and higher inaccuracy in the measurements. For example, finding the correct focus is challenging on the phase shift mask and can affect the recovered field (see Section 4.2).

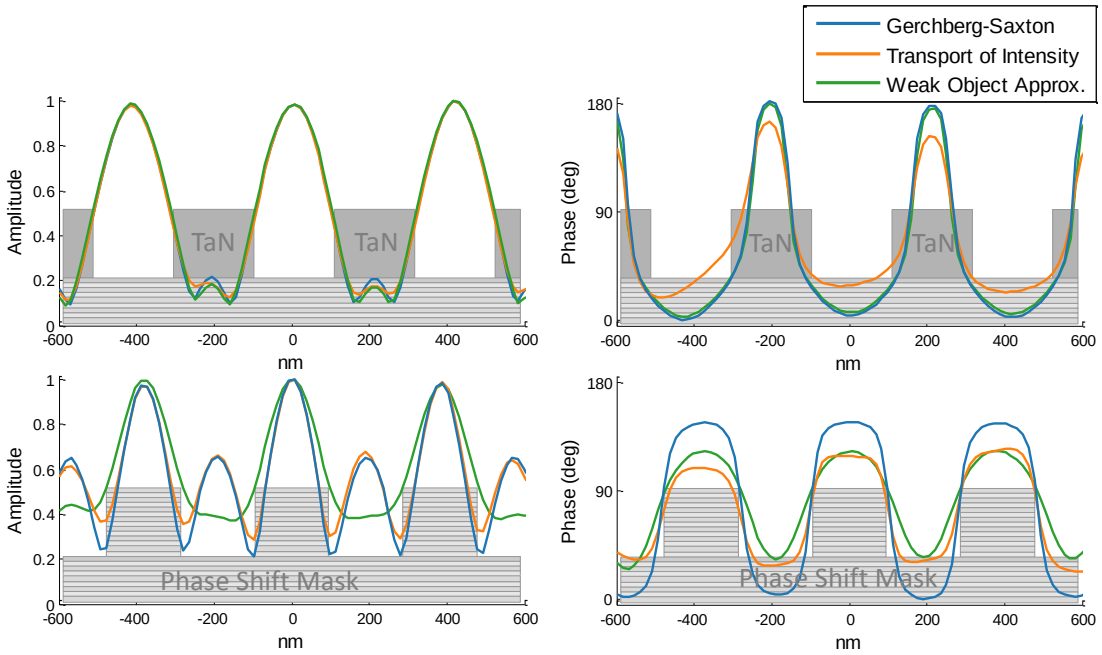

Figure 3: The recovered phase and amplitude using each of the algorithms is shown. For the TaN absorber the Transport of Intensity seems to have an error in the phase. For the phase shift mask both the Transport of Intensity and Weak Object Approximation seem to work poorly.

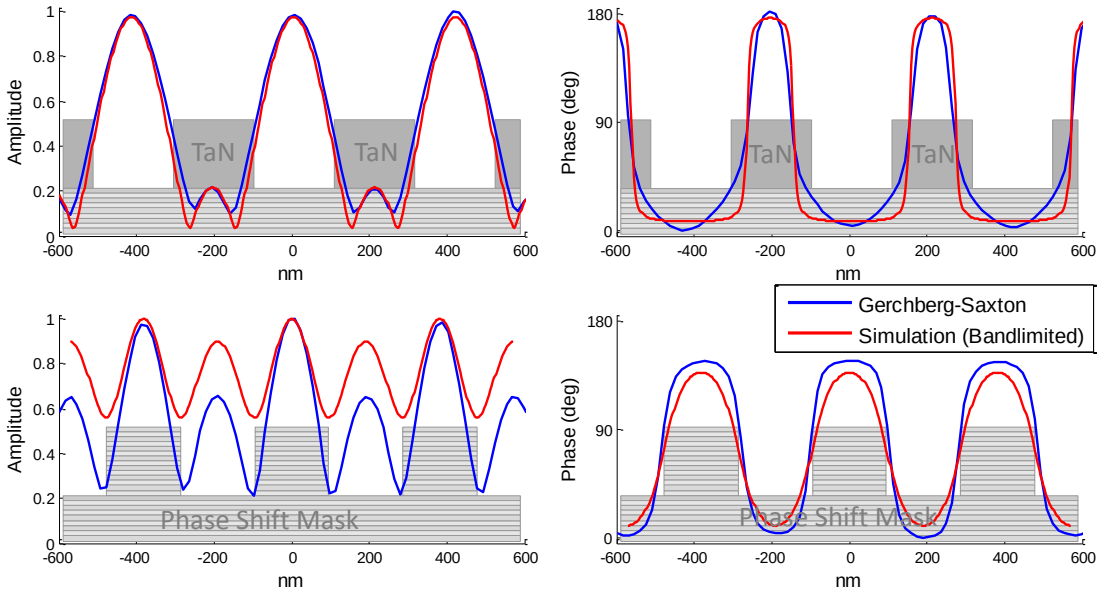

Figure 4: The simulated field from Figure 1 and the Gerchberg-Saxton result from Figure 3 are shown.

4. EFFECT OF MEASUREMENT ERRORS

There are a number of uncertainties that can arise when performing the measurements. For example, there may be an intensity offset—a background due to scattered light or dark current. Focus is difficult to determine under coherent illumination, especially for the phase shift mask where there is no obvious best focus image. Additionally, the illumination may not actually be fully coherent. Since phase retrieval is a non-linear process, the effect of these errors on the recovered field can be complicated. To evaluate the effect of some of these errors on the recovered field, we examine how the recovered field changes with different amounts of these errors.

4.1 Background

Dark current in the sensor or scattered light in the system can cause the signal of each pixel to be higher than it should be. We assume that this value is a single constant for all pixels. As the images are preprocessed for the phase retrieval algorithm a fixed background is subtracted. However, the intensity level of the background subtracted may not be correct. To consider the effect of this on the algorithms we apply the WOTF and GS phase retrieval algorithms (TIE is ignored since it is not producing an accurate result) to the measurements after removing different amounts of background. The recovered fields are shown in Figure 5. For the phase shift mask only the GS result is shown since the WOTF also failed. Background is defined as the percent of the mean intensity across all the images (after the correct background has been removed). So, for each recovered field, instead of subtracting a background of X, a background of $Y < X$ is subtracted.

From Figure 5 it is apparent that for the WOA the recovered field and amplitude are damped out. The phase difference decreases and the amplitude also decreases. The result of GS is significantly less sensitive to the background, however. This is to be expected since the WOA estimates the 0^{th} order using the mean intensity, and the background will bias that estimate.

4.2 Focus

Under coherent illumination the recovered field will describe the measurements equally accurately even if there is a global focus offset. This focus offset will change the recovered phase and amplitude, which can make the result appear more or less like the simulation result. To test this, different global focus offsets are used and the recovered field for each focus offset is shown in Figure 6. For the phase shift mask, the phase becomes less rectangular with negative defocus while the difference between the two amplitude peaks decreases. This qualitatively describes the discrepancy between the simulation and recovered field and highlights the difficulty and importance of determining the true focus position.

4.3 Coherence

The measured images were taken with coherent illumination. The actual illumination during the measurements, however, is probably not perfectly coherent. Figure 7 shows how the recovered field changes if partially coherent illumination is used. Unlike in Sections 4.1 and 4.2, in this section the input images to the algorithms are simulated to create different partial coherence. The field used in the simulations is the recovered field from Figure 4.

The GS algorithm is very sensitive to partial coherence and starts failing at $\sigma = 0.1$. While the WOTF can consider the effect of partial coherence and is expected to produce a more accurate recovery, it performs only slightly better. It fails for $\sigma > 0.2$. While it is not clear exactly why this happens, it may be because the transfer function is weaker under less coherent light. For coherent light the transfer function for phase can have a peak of 2. For less coherent light, the peak can decrease significantly. This could cause the I_s in Equation 1, which behaves like noise for the WOTF to dominate. Since the high contrast pattern was not a weak object to begin with, this could cause the algorithm to start failing.

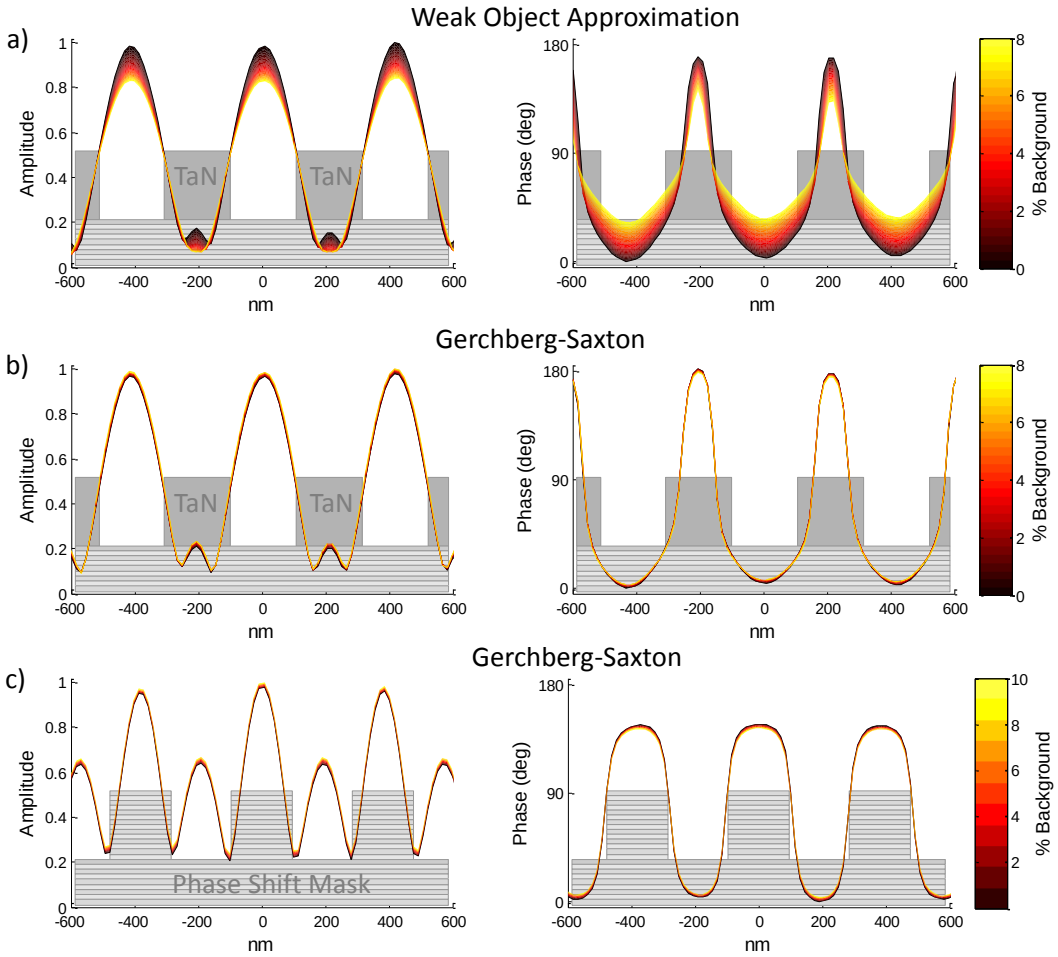

Figure 5: The recovered amplitude and phase are shown for different amounts of background in the images. The background is given as a percent of the mean intensity.

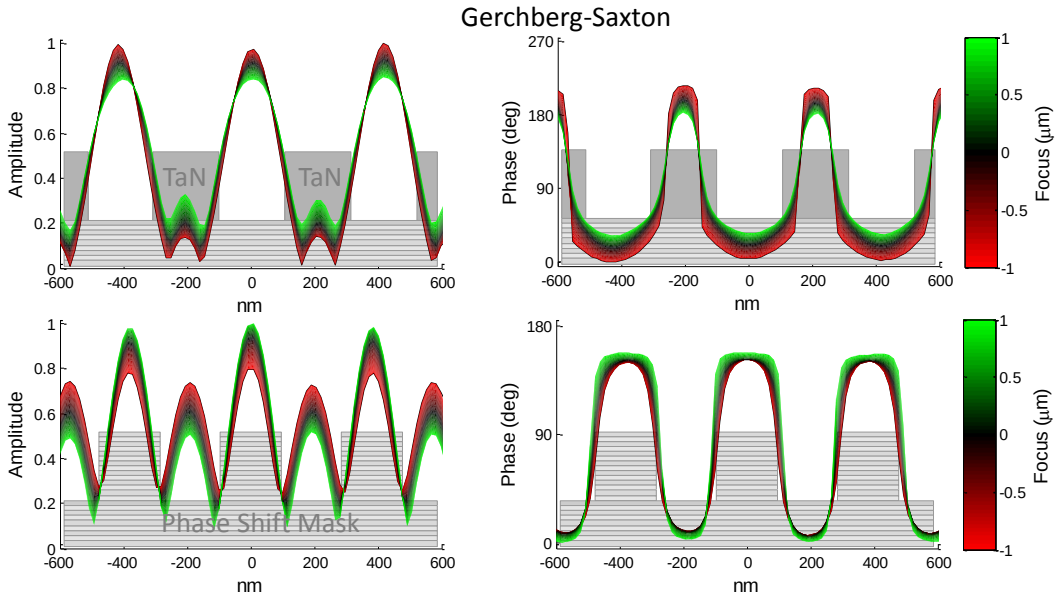

Figure 6: The recovered field under different global focus offsets is shown. The ±1 µm defocus corresponds approximately to 1 Rayleigh depth of focus. GS was used to recover these fields.

5. CONCLUSION

Three phase retrieval algorithms are evaluated for patterned EUV photomasks. Of the algorithms evaluated, the Gerchberg-Saxton algorithm was found to be the most reliable, though the Weak Object Transfer Function can also be applied when there is a strong 0^{th} order. Of the masks examined, the WOA works for the TaN absorber where the 0^{th} is only slightly reduced, but fails for the phase shift mask. The Transport of Intensity Equation failed to produce reasonable results on the data tested, though this may be because the implementation of TIE used only considered 3 images. The recovered field produced by GS approximately matched rigorous simulations, though it matched more closely for the TaN absorber than for the phase shift mask.

Evaluating measurement errors it is found that background intensity, such as from dark current in the sensor, can have significant effects on the WOTF algorithm, but has a relatively small effect on GS. Coherence uncertainty, on the other hand, is handled better by the WOTF since it can incorporate information about the source into the algorithm. Neither GS nor WOTF were able to handle source sizes larger than $\sigma = 0.2$. It is also shown that incorrectly specifying the correct focus offset can qualitatively change the phase and amplitude, which can make it challenging to compare results to simulation.

ACKNOWLEDGMENTS

This work performed in part at Lawrence Berkeley National Laboratory which is operated under the auspices of the Director, Office of Science, of the U.S. Department of Energy under Contract No. DE-AC02-05CH11231. This research was supported by collaboration with industry under the IMPACT+ program.

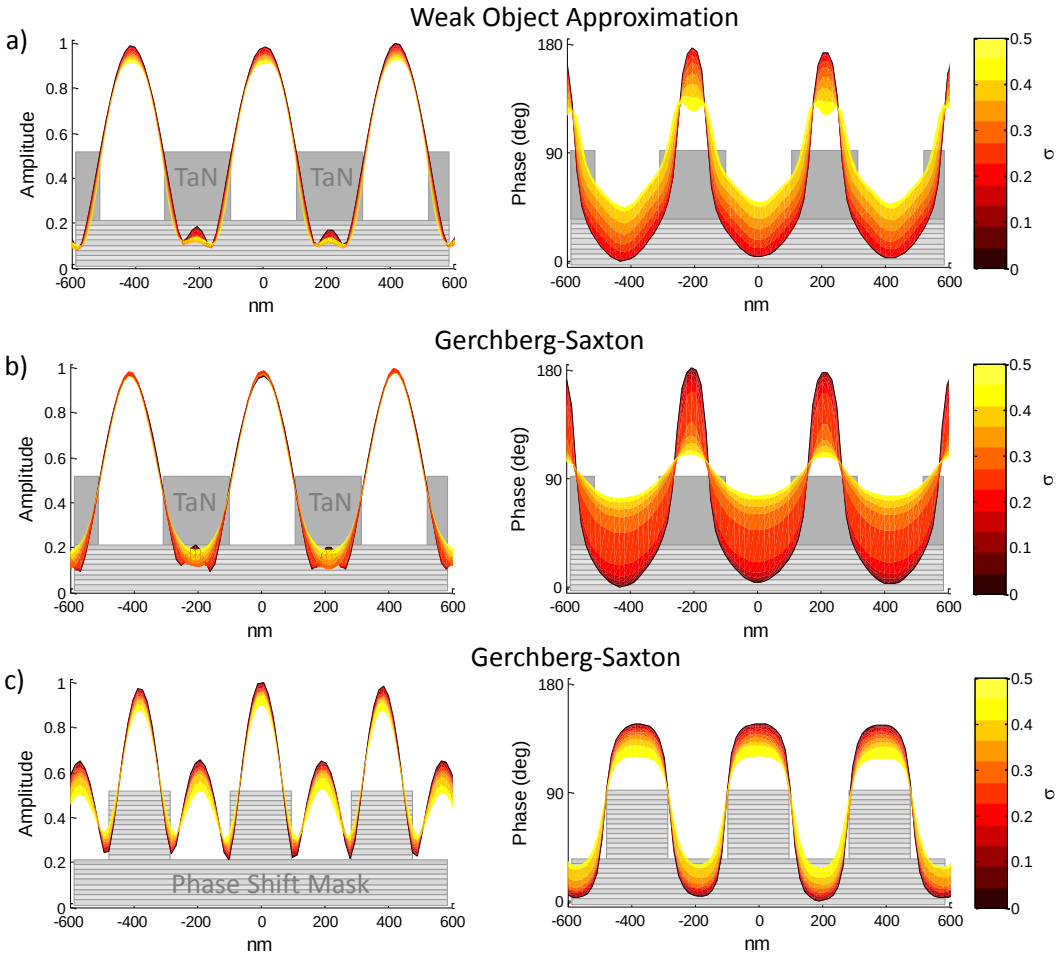

Figure 7: The recovered field is shown when the simulated images that are used as measurements use partially coherent illumination. The WOTF incorporates the correct coherence which is why it performs slightly better.

REFERENCES

[1] Shanker, A., Tian, L., Sczyrba, M., Connolly, B., Neureuther, A., and Waller, L., "Transport of intensity phase imaging in the presence of curl effects induced by strongly absorbing photomasks," *Applied Optics* **53**, J1–J6 (12 2014).

[2] Claus, R. A., Wang, Y.-G., Wojdyla, A., Benk, M. P., Goldberg, K. A., Neureuther, A. R., Naulleau, P. P., and Waller, L., "Phase measurements of EUV mask defects," *Proc. SPIE* **9422**, 942217 (2015).

[3] Gerchberg, R. W. and Saxton, W. O., "A Practical Algorithm for the Determination of Phase from Image and Diffraction Plane Pictures," *Optik* **35**(2) (1972).

[4] Reed Teague, M., "Deterministic phase retrieval: a Greens function solution," *Journal of the Optical Society of America* **73**(11), 1434 (1983).

[5] Claus, R. A., Naulleau, P. P., Neureuther, A. R., and Waller, L., "Quantitative phase retrieval with arbitrary pupil and illumination," *Optics Express* **23**(20), 26672 (2015).

[6] Goldberg, K. A., Mochi, I., Benk, M., Allezy, A. P., Dickinson, M. R., Cork, C. W., Zehm, D., Macdougall, J. B., Anderson, E., Salmassi, F., Chao, W. L., Vytla, V. K., Gullikson, E. M., DePonte, J. C., Jones, M. S. G., Van Camp, D., Gamsby, J. F., Ghiorso, W. B., Huang, H., Cork, W., Martin, E., Van Every, E., Acome, E., Milanovic, V., Delano, R., Naulleau, P. P., and Rekawa, S. B., "Commissioning an EUV mask microscope for lithography generations reaching 8 nm," *Proc. SPIE* **8679**, 867919 (2013).

[7] Jingshan, Z., Tian, L., Claus, R. A., Dauwels, J., and Waller, L., "Partially Coherent Phase Recovery by Kalman Filtering," in [*Frontiers in Optics 2013 Postdeadline*], FW6A.9, OSA (10 2013).

[8] Jingshan, Z., Tian, L., Dauwels, J., and Waller, L., "Partially coherent phase imaging with simultaneous source recovery," *Biomedical Optics Express* **6**(1), 257–65 (2015).

[9] Jingshan, Z., Claus, R. A., Dauwels, J., Tian, L., and Waller, L., "Transport of Intensity phase imaging by intensity spectrum fitting of exponentially spaced defocus planes," *Optics Express* **22**(9), 10661–74 (2014).

[10] http://panoramictech.com/.